Proc. IEEE Trans. Nucl. Sci.
November 8-14, 1998
Toronto, Canada

BNL-66886

The 15 layer Silicon Drift Detector Tracker in Experiment 896. [1]

S.U. Pandey[2], R. Bellwied[2], R. Beuttenmueller[3], H. Caines[4], W. Chen[3], D. DiMassimo[3], H. Dyke[4], D. Elliot[3], M. Grau[3], G.W. Hoffmann[5], T.J. Humanic[4], P. Jensen[5], I.V. Kotov[4,a], H.W. Kraner[3], P. Kuczewski[3], W. Leonhardt[3], Z. Li[3], C.J. Liaw[3], G. Lo Curto[4], D. Lynn[3], P. Middelkamp[3], R. Minor[6], S. Nehmeh[2], G. Ott[5], D. Pinelli[3], C. Pruneau[2], V. Rykov[2], J. Schambach[5], J. Sedlmeir[3], J. Sheen[2], R. Soja[3], D. Stefani[3], E. Sugarbaker[4], J. Takahashi[2,b], W.K. Wilson[2]

(STAR-SVT collaboration)

[2]Wayne State University, Detroit, MI 48201, USA

[3]Brookhaven National Laboratory, Upton, NY 11973, USA.

[4]The Ohio State University, Columbus, OH 43210, USA.

[5]University of Texas, Austin, TX 78712, USA.

[6]Lawrence Berkeley National Laboratory, CA 94720, USA.

[a]Institute for High Energy Physics, Protvino, Russia 142284

[b]Universidade de Sao Paulo, Sao Paulo, BR.

Abstract

Large linear silicon drift detectors have been developed and are in production for use in several experiments. Recently 15 detectors were used as a tracking device in BNL-AGS heavy ion experiment (E896). The detectors were successfully operated in a 6.2T magnetic field. The behavior of the detectors, such as drift uniformity, resolution, and charge collection efficiency are presented. The effect of the environment on the detector performance is discussed. Some results from the experimetal run are presented. The detectors performed well in an experimental enviromental. This is the first tracking application of these detectors.

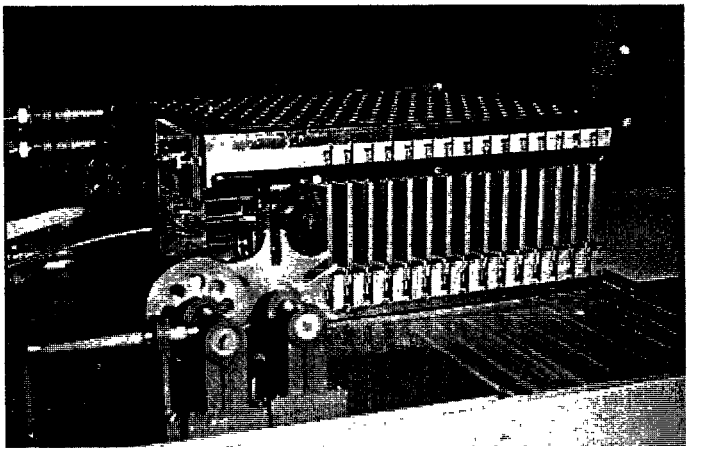

Fig. 1 An array of 15 silicon drift detectors used in experiment 896.

I. INTRODUCTION

A Silicon Drift Detector (SDD) is a charged particle position-measuring device with a position resolution on the order of 10 microns in each coordinate[1, 2]. A charged particle crossing the detector creates electron-hole pairs. Cathodes on the surface of the detector immediately absorb the holes. Electrons converge to the middle of the detector and drift at a constant speed under the influence of an applied uniform electric field toward low capacitance anodes located near the edge of the silicon wafer. One coordinate of the particle position is determined from the drift time while charge division between anodes provides the other coordinate.

Large (6.3x6.3cm^2) linear Silicon Drift Detectors (SDD) have been developed and are in production for use in the Silicon Vertex Tracker (SVT), the inner tracking detector of the STAR experiment at the RHIC Collider[3]. A 15 layer SDD has been used in a heavy ion fixed target experiment (E896) at the AGS-Brookhaven National Laboratory. Statistically significant statements about the detector's properties and behavior in experimental environments can now be made. Constraints and features of the performance of these detectors are important to know since these detectors are being used to extract weak experimental signatures from data. A discussion of the criteria and requirements used to select detector wafers (test structures, probe stations, yields) is presented. The behavior of the detectors, such as drift uniformity, resolution, and charge collection efficiency is discussed. Environmental influences on the detectors such as temperature, high-voltage bias, and magnetic field are presented.

We shown that the latest detector design for the SDD exhibits good performance and meets the specification requirements for the SVT project.

II. EXPERIMENT 896

Experiment 896 is a heavy-ion fixed target experiment measuring Au^{197} + Au^{197} collisions at 11.6 GeV/c per nucleon at the AGS collider at Brookhaven National Laboratory[4]. The experiment searches for the H0 dibaryron and has high sensitivity for short-lived particles due to an array of STAR/SVT SDD's which sits close to the interaction point, thus allowing good charged particle tracking and vertexing. The array, seen in fig. 1 sat in a 6.2T magnetic field and was

[1]Author:Ph.(1)516-344-6151,email.sanjeev@bnl.gov.

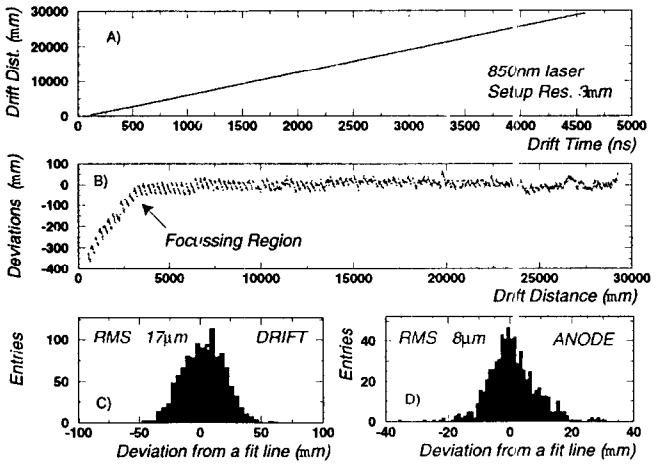

Fig. 2 Figure A plots the drift time vs drift distance curve generated as a laser scans across the surface of the detector. Figure B shows deviations from a quadratic line fit to Figure A. Figure C is a projection of Figure B onto its Y axis for drift distances larger than 3mm. Figure D is similar to Figure C but along the anode direction.

operated at a temperature 35C and a drift field of 500V/cm. The detectors are 6.3x6.3 cm^2 and are divided into two symmetrical drift directions each having 240 anodes at 250 micron pitch. The active area of the detector is 94.5%.

III. Detector Selection

Wafers are thoroughly tested before being selected for use in experiment 896. The testing procedure has been described in detail in Ref. [5] before. The wafers are visually inspected for electrical bridges between structures and mask misalignments. Wafers that pass the above inspection have their test structures situated at the edge of the wafer measured. These diodes and implanted resistor chains provide valuable input on breakdown voltages of the resistors, the actual value of the resistors, and p-n junction reverse bias currents. The next stage involves testing the detector on the wafer. Probes on both sides of the wafer make electrical contact with cathodes and anodes. The wafer is biased to 1000V and the voltage linearity, guard anode currents, and anode currents are measured. Wafers with large voltage non-linearities or large currents are rejected. Production yields around 75% are currently achieved[6]. Selected wafers are then cut with a laser and bonded onto printed circuit boards that hold them and their readout electronics. A p+ implant, surrounding and capacitively coupled to the anodes, is then pulsed and the detector is read out. This allows one to check for dead channels in the readout electronics. Finally the response of each anode is checked via laser injection (850nm) at long drift. There were less than 1% dead channels for the 15 detectors selected for experiment 896.

IV. Position Resolution and Calibrations

It is useful to distinguish between the intrinsic resolution of the 280 microns thick detector, and the resolution of the detector for minimum ionizing particles (MIP) which are additionally influenced by noise since they have low signal

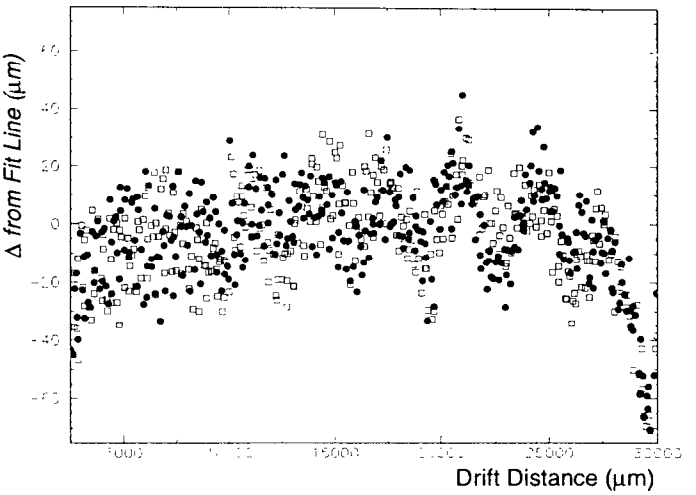

Fig. 3 Two different measurements of the same drift nonlinearities.

amplitude. An XY stage with a resolution of 1 micron moves an 850nm laser across the surface of the detector. Vibrations and small temperature fluctuations in the setup limit the intrinsic single point measuring accuracy to 4 microns. This is determined by laser injection at the same spot on the detector and plotting the resulting spread in positions. For this measurement the signal on the detector was large so the effect of noise can be neglected. The single point position accuracy of MIP's is influenced by noise and is around 15 microns. Along the drift direction the linear relationship between drift distance and drift length is affected by nonlinearities in the drift field caused by non-homogeneous implanted resistors. This adversely affects the intrinsic position resolution as seen in fig. 2. One measure of the position resolution is obtained by fitting the drift distance vs. drift time data and plotting deviations from the fit as seen in fig. 2B. The intrinsic resolution of about 20 microns along drift is larger than that of 10 microns along the anodes due to drift nonlinearities. For MIP hits the resolutions are 25 microns along drift and 15 microns along the anodes. Similar figures are obtained for the 19 other detectors tested. Fig. 3 shows two independent

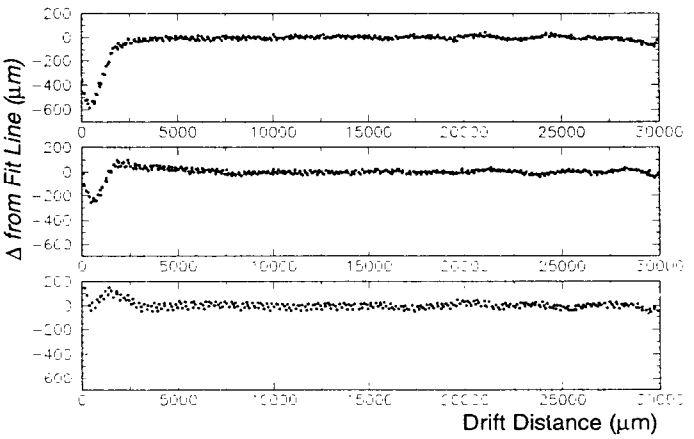

Fig. 4 Adjusting the top and bottom side of the detector's voltages can dramically change the drift linearity.

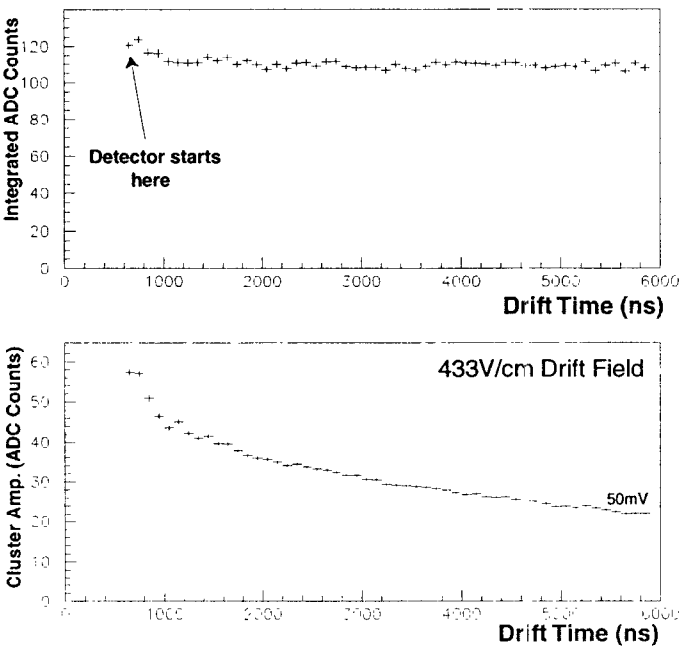

Fig. 5 The amplitude of a MIP hit decreases with drift distance due to diffusion but the total change remains constant. At 500V/cm the MIP amplitude at 3cm drift is 70mV.

calibration measurements made on the same detector that demonstrate that the nonlinearities to a large extent match. This implies that these nonlinearities are calibratable and the achievable position resolution is better than that show in fig. 2. For experiment 896, drift distance vs. drift time curves are measured for each detector. Knowing the drift time allows one to read off the drift distance for a given drift velocity. Results for different anodes on a detector are very similar. Thus measuring a few anodes is sufficient to "map" a detector[2].

Around a drift distance of 2.5 mm there is a change in the drift velocity caused by a voltage difference between the top and bottom side of the detector to force the drifting electrons to be collected at anodes which lie at the surface of the detector. Adjusting these voltages, as seen in fig. 4, can minimize the

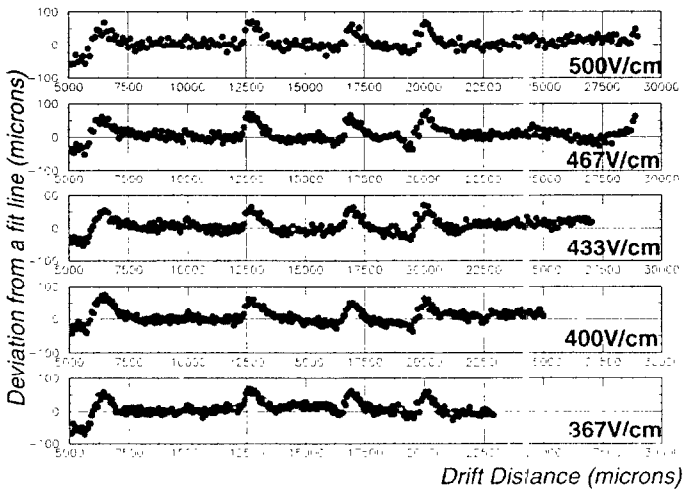

Fig. 6 Differential nonlinearities as a function of drift field.

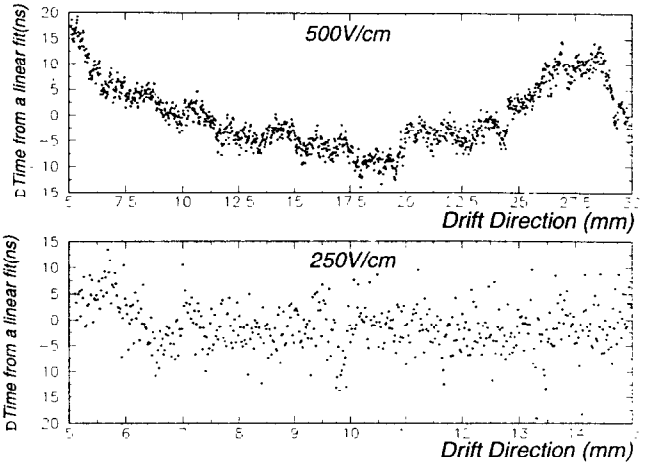

Fig. 7 Leakage currents at the cathodes create slight parabolic drift potentials at high drift fields.

magnitude of this change. Some care has to be taken when adjusting these voltages to optimize charge collection as it is possible to lose part of the cloud on non-anode structures on the surface[7].

A simple simulation was run mimicking our detector's noise, MIP hits and readout electronic response. The resulting signals were fit to determine what is the expected position resolution. Results are consistent with our measurements. These simulations indicate that improvements in the position resolution can be made by sampling in smaller bins along the drift direction as the signal width approaches the bin width for short drift distances.

V. Environmental Effects

The detector's response is sensitive to certain environmental conditions such as the drift electrical field, the temperature, and the external magnetic field. Changing the drift field changes the total drift time in inverse proportion, as expected. Longer drift times mean more diffusion and thus the signal's amplitude decreases as the signal's width increases as seen in fig. 5. This can be problematic when one works in noisy environments. Larger signal widths also degrade the two hit separation of the detector[9]. Further, longer drift times increase the dead time of the detector which is a disadvantage when running in high luminosity experimental environments. At 500V/cm the dead time (total drift time) of the detector is 4.7 μs. As one reduces the high voltage the magnitude and position of the nonlinearities remain constant as seen in fig. 6. This is consistent with the nonlinearities being caused by the implanted resistor chain. This trend will not continue indefinitely as at very low drift fields the region around the anodes will no longer be fully depleted decreasing the signal to noise which impacts ones position resolution. One additional effect of large drift fields is that cathodes start to leak at large fields (at the p+ implant edges) causing parabolic drift potentials. These can be minimized by using small values for the implanted resistors. For the 500 KOhm resistors used on the STAR/SVT detectors the effect can be seen in fig. 7 and

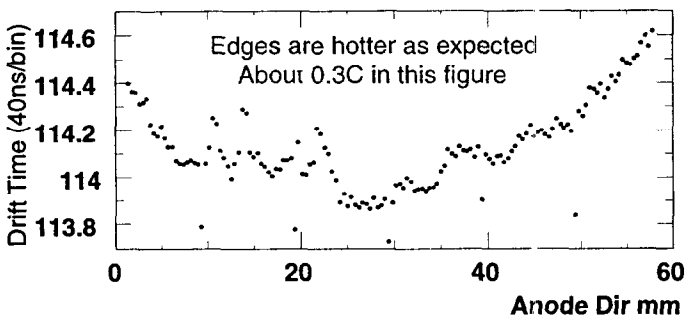

Fig. 8 The edges of the wafers are hotter than the center.

is small and easily calibrated away by using quadratic fits.

Changes in temperature change the carrier concentration and the thermal average velocity of electrons. Including all scattering mechanisms at room temperature[10] the drift velocity changes by 1% for each Kelvin increase in temperature. There is a temperature profile across the detector caused by the implanted resistor chains on either edge of the detector. The edges of the detector are hotter than the center. This can be seen by moving the laser across the anodes at a fixed drift distance from the anodes. Any change in the drift time will be caused by changes in the local temperature and the result is shown in fig. 8. The dip in the center of the wafer corresponds to about a 0.3K temperature difference agreeing with expectations from a finite element calculation[8].

Finally the magnetic field (B) can dramatically affect the detectors response[11, 12]. B fields perpendicular to the drift direction and out of the plane of the detector will cause the electrons to drift at an angle determined by the Hall coefficient as they drift towards the anodes. B fields perpendicular to the drift direction and parallel to the plane of the detector cause the

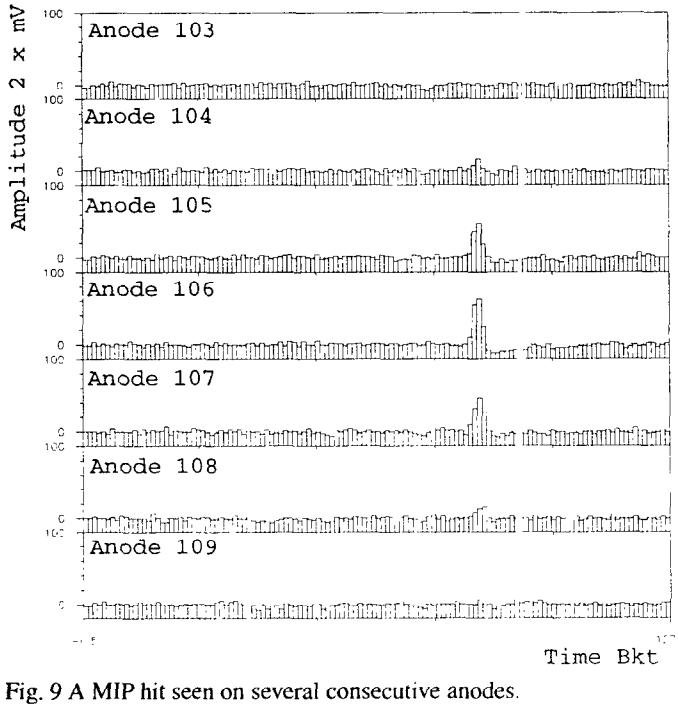

Fig. 9 A MIP hit seen on several consecutive anodes.

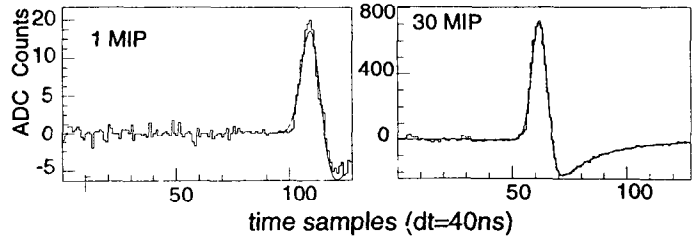

Fig. 10 The dynamic range of the detector response changes with drift distance due to difussion of the electon cloud.

electrons to no longer drift in the center of the wafer. Finally a B field parallel to the drift direction while not directly affecting the motion of the electrons changes the resistance of silicon (magneto-resistance) and thus decreases the drift speed of the electrons. In experiment 896 which ran at a B field of 6.2T parallel to the drift direction this effect was measured and found to reduce the drift velocity by about 10%. Since a reversal of the B field should cause the same behavior, this effect must be proportional to B^2 on symmetry grounds. Data are now being analyzed.

VI. Signals

The longer the drift time, the more the electrons diffuse and the signal width increases as the square root of the drift time. This lowers the amplitude but the integrated charge in the signal is constant as seen in fig. 5. A typical MIP signal is shown in fig. 9. Hits are easy to extract due to the low noise on the detector[13]. The undershoot at large time is caused by the readout electronics bipolar response function which reduces baseline shifts in large multiplicity environments. The signal to noise ratio can be calculated by summing over the

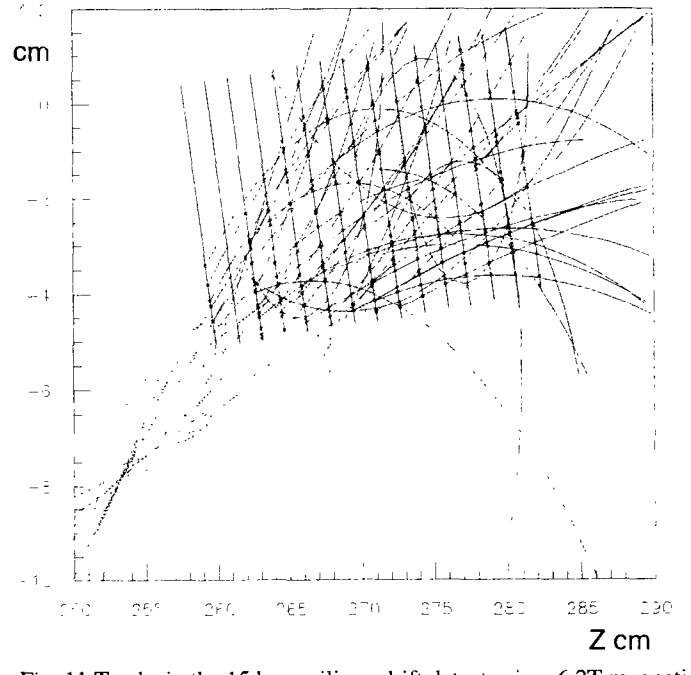

Fig. 11 Tracks in the 15 layer silicon drift detector in a 6.2T magnetic field.

amplitude of the pixels in the hit and dividing by the square of the number of pixels times the noise on one pixel. It is about 20 for the operating conditions of this detector decreasing slightly for longer drift distances.

In experiment 896 a large distribution of pulse heights from one to many MIP hits was seen. The dynamic range of the detector changes with drift distance as large hits have smaller amplitudes at long drift due to diffusion as seen in fig. 10. Typically there were about 60 hits/plane in experiment 896 which corresponds to a 2% occupancy on the detector. While alignment calibrations are still being finalized and drift and magnetic field velocity calibrations have yet to be implemented, preliminary tracking results are presented in fig. 11. Residuals from these plots are 200 microns along the drift and 100 microns along the anodes. Residuals are worse along the drift direction since drift calibrations and B field corrections are yet to be implemented.

VII. Conclusions

The first tracking device based on silicon drift detectors has been built and operated successfully. Yields from these detectors are high at around 75%. The detectors have good position resolution but calibration schemes need to be implemented carefully to get the best performance from these detectors. The detectors perform well in magnetic fields as large as 6.2T. There were less than 1% dead channels in the whole array of 15 detectors. The technology for making and using large silicon drift detectors as tracking devices is now mature.

VIII. Acknowledgements

We are grateful for the partial support given by the US Department of Energy through grant DE-FG02-93ER40795, RHIC R&D (STAR) funds, the Robert A. Welch Foundation, and the National Science Foundation through grant PHY-9511850.

IX. References

[1] E Gatti, P Rehak and J Walton "Silicon drift detectors - First results and optimum processing of signals", *Nucl. Instr. and Meth., vol. 226, 1984* pp. 129-141.

[2] R Bellwied, R Beuttenmueller, W Chen, D DiMassimo, L Dou, H Dyke, A French, J R Hall, G W Hoffmann, T Humanic, I Kotov, H W Kraner, C J Liaw, D Lynn, S Paganis, L Ray, D Read, V L Rykov, S U Pandey, C Pruneau, J Schambach, J Sedlmeir, G Vilkelis and W K Wilson "Development of large linear silicon drift detectors for the STAR experiment at RHIC", *Nucl. Instr. and Meth., vol. A377, 1996* pp. 387-392.

[3] J W Harris and the STAR Collaboration "The STAR experiment at the relativitic heavy ion collider," *Nucl. Phys., vol. A566, 1994* pp. 277c.

[4] W J Lope and the E896 Collaboration "The BNL-AGS experiment 896", *12th Winter Workshop on Nuclear Dynamic Proceedings, 1996* Snowbird, Utah, Plenum Press, NY.

[5] J Takahashi, R Bellwied, R Beuttenmueller, H Caines, W Chen, D DiMassimo, H Dyke, D Elliot, M Grau, G W Hoffmann, T Humanic, P Jenson, I V Kotov, H W Kraner, P Kuczewski, W Leonhardt, Z Li, C Liaw, G LoCurto, D Lynn, N Mazeh, P Middelkamp, R Minor, S Nehmeh, G Ott, S U Pandey, D Pinelli, C Pruneau, V L Rykov, J Schambach, J Sedlmeir, J Sheen, R Soja, D Stefani, E Sugarbaker and W K Wilson "Silicon drift detectors for the STAR/SVT experiment at RHIC,", *8th European Symposium of Semiconductor Detectors, 1998* Schloss Elmau, Germany. Submitted.

[6] http://www.rhic.bnl.gov/ sanjeev/svt1.html

[7] R Bellwied, R Beuttenmueller, W Chen, D DiMassimo, L Dou, H Dyke, A French, J R Hall, G W Hoffmann, T Humanic, I V Kotov, H W Kraner, Z Li, C J Liaw, J Lopez, D Lynn, V L Rykov, S U Pandey, C Pruneau, J Schambach, J Sedlmeir, E Sugarbaker, J Takahashi and W K Wilson "Anode region design and focussing properties of STAR silicon drift detectors", *Nucl. Instr. and Meth., vol. A400, 1997* pp. 279-286.

[8] C J Liaw. Private Communication.

[9] S U Pandey, , R Bellwied, R Beuttenmueller, H Caines, W Chen, D DiMassimo, H Dyke, J Hall, G W Hoffmann, T Humanic, I V Kotov, H W Kraner, P Kuczewski, W Leonhardt, Z Li, C Liaw, G LoCurto, D Lynn, P Middelkamp, G Ott, C Pruneau, V L Rykov, J Schambach, J Sedlmeir, J Sheen, R Soja, E Sugarbaker, J Takahashi and W K Wilson "Measurement of two particle resolution in silicon drift detectors", *IEEE Trans. on Nucl. Sci., vol. 45, no. 3, 1998* pp. 315-321.

[10] S M Sze "Physics of Semiconductor Devices", *New York: Wiley, 1981* ch. 1.

[11] S U Pandey, D Cooper, H Dyke, D Elliot, T J Humanic, J Kirkman, I V Kotov, G Lo Curto, E Sugarbaker, G Vilkelis, R Bellwied, L Dou, A French, J Hall, C Pruneau, V Rykov, J Takahashi, W K Wilson, R Beuttenmueller, W Chen, D DiMassimo, H W Kraner, C J Liaw, D Lynn, J Sedlmeir, G W Hoffmann, S Paganis, and J Schambach "Behavior of silicon drift detectors in large magnetic fields", *IEEE Transactions on Nuclear Science, vol. 44, 1997* pp. 610-614.

[12] A Castoldi, E Gatti, V Manzari, P Rehak "Performance of silicon drift detectors in a magnetic field", *Nucl. Instr. and Meth., vol. A399, 1997* pp. 227-243.

[13] D Lynn, R Bellwied, R Beuttenmueller, H Caines, W Chen, D DiMassimo, H Dyke, D Elliot, M Grau, G W Hoffmann, T Humanic, P Jenson, S A Kleinfelder, I V Kotov, H W Kraner, P Kuczewski, W Leonhardt, Z Li, C Liaw, G LoCurto, P Middelkamp, N Mazeh, R Minor, S Nehmeh, P O'Conner, G Ott, S U Pandey, D Pinelli, V Radeka, S Rescia, C Pruneau, V L Rykov, J Schambach, J Sedlmeir, J Sheen, R Soja, D Stefani, E Sugarbaker, J Takahashi and W K Wilson "A 240-channel thick film multi-chip module for readout of silicon drift detectors", *8th European Symposium of Semiconductor Detectors, 1998* Schloss Elmau, Germany. Submitted.